High-resolution calorimetric study of the nematic to smectic-*A* transition in aligned liquid crystal–aerosil gels

F. Cruceanu,[1] D. Liang,[2] R. L. Leheny,[2] C. W. Garland,[3] and G. S. Iannacchione[1,*]
[1]*Department of Physics, Worcester Polytechnic Institute, Worcester, Massachusetts 01609, USA*
[2]*Department of Physics and Astronomy, Johns Hopkins University, Baltimore, Maryland 21218, USA*
[3]*Department of Chemistry, Massachusetts Institute of Technology, Cambridge, Massachusetts 02139, USA*
(Received 6 June 2008; published 29 January 2009)

High-resolution ac calorimetry has been used to study the nematic to smectic-*A* (*N*-Sm*A*) phase transition in the liquid crystal octylcyanobiphenyl (8CB) confined in aligned colloidal aerosil gels. A stable and robust nematic alignment was achieved by repeated thermal cycling of the samples in the presence of a strong uniform magnetic field. In some ways (such as transition temperature and integrated enthalpy), the dependence of the specific heat peak associated with the *N*-Sm*A* transition on the aerosil density for aligned gels is consistent with that observed in unaligned (random) gel samples. However, a power-law analysis reveals that the behavior of the critical exponent α is quite different. For random gels, α varies gradually with aerosil density, whereas we find that α for aligned gels shifts abruptly to an *XY*-like value for the lowest aerosil density studied and remains essentially constant as the sil density increases. This aerosil density independence of α is consistent with the critical behavior of the smectic correlation lengths obtained from an x-ray scattering study of 8CB in aligned aerosil gels. The combined calorimetric and x-ray results indicate that the role of quenched randomness in aligned gels of 8CB+sils differs significantly from that in random gels.

DOI: 10.1103/PhysRevE.79.011710 PACS number(s): 64.70.mj, 61.30.Eb, 65.40.Ba

I. INTRODUCTION

The role of quenched random disorder (QRD) in perturbing second-order phase transitions is an actively investigated and important problem in condensed matter physics. The introduction of new, disorder-driven, critical behavior is of particular interest for the theory of critical phenomena for amorphous and pure systems. Soft-condensed matter systems have provided considerable insight into the physics of QRD beyond the work in doped magnetics [1] and superfluids in aerogels [2]. Work with a dilute aerogel glass matrix embedded in a liquid crystal provided an early advance but these systems were difficult to work with and appear to be in the strong disorder regime [3]. There remain many issues regarding QRD to be resolved, such as the onset of glassy behavior and the proper measure of disorder strength.

Low density thixotropic gels formed by dispersing aerosil nanoparticles in a liquid crystal (LC+gel), although originally explored for potential applications [4–6], provide excellent systems for the study of quenched disorder [7–9]. The focus of this work is on the nematic (*N*)–smectic-*A* (Sm*A*) transition, and the *N*-Sm*A* critical behavior of pure LCs has been extensively studied with high-resolution calorimetric and x-ray scattering techniques [10]. The colloidal gels formed by hydrogen-bonded cross-linked chains of aerosil particles create disorder due to surface interactions ("pinning") with LC molecules. It is expected theoretically [11] that such gels can introduce both random orientational fields that couple to the LC nematic director and random positional fields coupled to the smectic density-wave order parameter. Several random LC+sil systems have been investigated [12–15], and the most detailed random aerosil gel studies are on 8CB+sil samples [12,13,16,17]. Octylcyanobiphenyl (8CB) is a readily available and very stable liquid crystal, and the *N*-Sm*A* transition has been more extensively studied in 8CB than in any other LC.

Recently there has been reported a detailed x-ray study of 8CB confined in aligned (uniaxially strained) aerosil gels [18,19]. This anisotropic random environment is of special interest since there are theoretical suggestions [20] that smectics in an aligned gel should belong to the random-field *XY* universality class. This is in contrast to the case of LCs in random (unaligned) gels, where coupling of the orientational random fields to the nematic order parameter and the soft elasticity of the LC lead to the prediction [11] that the confined smectic phase is more complex and differs from standard random-field *XY* systems. For 8CB in aligned gels the low-temperature x-ray scattering intensity has been shown to be consistent with a *XY* Bragg glass [19]. Also the critical behavior of the smectic correlation lengths and susceptibility associated with thermal fluctuations in the nematic phase of aligned 8CB gels is different from that observed in random 8CB+sil gels. It should be noted that although both aligned and random gels destroy the quasi-long-range Sm*A* order observed in pure LCs [13,19] substantial short-range smectic order exists at low temperatures for LC+sils and thermal fluctuations can still be characterized by effective critical exponents.

The present paper describes a high-resolution calorimetric study of the heat capacity C_p associated with the *N*-Sm*A* transition in 8CB confined in aligned aerosil gels. These C_p data (corresponding to critical fluctuations in the enthalpy) complement data on the correlation lengths obtained from the x-ray study. By combining calorimetric and x-ray data, it is possible to demonstrate the applicability of two general concepts to 8CB in aligned gels–hyperscaling, which relates critical exponent values, and two-scale universality, which

*gsiannac@wpi.edu

concerns the magnitudes of the C_p peak and the correlation volume. Specifically, this work demonstrates the rapid crossover of the critical exponent α to *XY*-like critical behavior for the *N*-Sm*A* transition in aligned aerosil gels. These observations are discussed in terms of modification of the nematic-smectic coupling by the aerosil gel. More broadly, these results point to the unique ability of LC+gel systems to tune the nature of the quenched random disorder through the alignment of the aerosil gel.

The sample preparation and gel alignment procedures as well as the essential features of the ac-calorimetric technique are described in Sec. II. The experimental C_p results and the analysis of C_p in terms of critical exponents are given in Sec. III together with a general discussion general of the critical behavior of both C_p and the smectic correlation lengths. A discussion of the role of the gel in modifying the thermal fluctuations from those observed in the pure LC is given in Sec. IV.

II. EXPERIMENTAL PROCEDURES

Random gel samples of 8CB+sils were prepared using the solvent-dispersion method [12]. The liquid crystal octylcyanobiphenyl (8CB) was obtained from Frinton Laboratories and has a molar mass of 291.44 g mol^{-1}. The hydrophilic type-300 aerosil obtained from DeGussa consists of 7-nm diameter silica particles and has a specific area a of 300 m g^{-1}. Both materials were thoroughly degassed at high temperatures under vacuum for at least 2 hours. After measured amounts of 8CB and sil were dissolved and/or dispersed in high-purity (very low water content) acetone, the solvent was allowed to evaporate slowly over several hours. The resulting 8CB+sil gel was then degassed at ~320 K for 2–3 hours to ensure complete removal of the acetone. The concentration of the aerosil in each sample is characterized by a density ρ_S, defined as the mass of silica in grams per volume of LC in cm^3 (the units g cm^{-3} for ρ_S will be dropped hereafter). This definition of the sil density is useful since ρ_S can be directly related to important features of the gel such as the mean void size $l_0=2/a\rho_S$ and the pinning fraction $p=l_b a\rho_S$ (volume fraction of LC in a boundary layer contacting the solid surfaces where l_b is the layer thickness taken as the LC molecular length) [12,17,21]. Six different 8CB+sil batches were prepared with ρ_S values ranging from 0.030 to 0.150. The resulting 8CB+sil samples have a homogeneous aerosil gel structure that is fractal in character over a range of length scales [12,22] and such a gel is considered to be a random sample.

Aligned gel samples were prepared by sealing a random gel of the desired composition into a calorimetric cell and then thermally cycling the system ~100 times through the nematic-isotropic (*N*-*I*) phase transition in the presence of a 2-T magnetic field. The resulting aligned gel samples were robust and of good quality, as confirmed by x-ray studies of aligned samples that were prepared is a nearly identical way [18,19]. The C_p peaks were reproducible on repeated runs, and the x-ray work showed that the induced nematic alignment was unchanged by heating into the isotropic phase and then recooling in the absence of the magnetic field or by long-term storage at room temperature.

High-resolution ac calorimetric data were acquired using a home-built calorimeter whose basic characteristics have been described elsewhere [23]. The technique consists of applying a very low frequency ac heating power to the cell as $P_{ac}e^{i\omega t}$ and detecting the amplitude of the resulting temperature oscillations T_{ac} and a relative phase shift of $\varphi=\Phi+\pi/2$, where Φ is the absolute phase shift between $T(\omega)$ and the input power. The specific heat at a heating frequency ω is given by

$$C_p = \frac{(C'_{\text{filled}} - C_{\text{empty}})}{m_{\text{LC}}} = \left(\frac{P_{ac}}{\omega |T_{ac}|} \cos\varphi - C_{\text{empty}} \right) \Big/ m_{\text{LC}}, \tag{1}$$

$$C''_p = \frac{C''_{\text{filled}}}{m_{\text{LC}}} = \left(\frac{P_{ac}}{\omega |T_{ac}|} \sin\varphi - \frac{1}{\omega R} \right) \Big/ m_{\text{LC}}, \tag{2}$$

where C'_{filled} and C''_{filled} are the real and imaginary components of the sample+cell heat capacity, C_{empty} is the heat capacity of the cell and the silica, m_{LC} is the mass in grams of the liquid crystal (since the total mass of 8CB+sil was ~15 mg, the m_{LC} values lie in the range 10–15 mg), and R is the thermal resistance between the cell and the bath (typically 200 K W^{-1}). Measurements were conducted at various frequencies in order to confirm the applicability of Eqs. (1) and (2) by checking that $C''_p \approx 0$ through the *N*-Sm*A* transition region and that C_p was independent of ω. Finally, a small, essentially *T*-independent, correction factor is required to account for the finite internal thermal resistance compared to the external R, and this correction (on the order of 0.5% for both aligned and random samples) was applied to all samples [24]. Note that in these measurements, the silver cell completely encloses the aligned 8CB+sil sample resulting in two parallel thermal paths from the heater to thermometer. Any change in the thermal resistance of the 8CB+sil sample due to alignment will not dominate that of the silver cell, and thus the applicability of this one-lump model is ensured over the entire temperature range studied.

All data presented here were taken at $\omega=0.1473$ s^{-1} and the scanning rate for the variation in the mean sample temperature was less than ± 200 mK h^{-1}, which yields essentially static C_p values. All 8CB+sil samples underwent the same thermal history after being mounted in the calorimeter: six hours in the isotropic phase to ensure equilibrium in such samples where disorder can induce slow dynamics [25,26], then a slow cool deep into the smectic phase before beginning initial data collection during slow heating.

In addition to the six aligned gel samples, two random gels (with $\rho_S=0.05$ and 0.13) were also studied in order to provide confirmation that the 8CB sample and calorimetric procedures were completely compatible with previously presented results [12]. We note that these reference samples were subjected to a thermal history identical to that of the aligned gels; specifically, they were cycled between the isotropic and nematic phases ~100 times while positioned in the bore of the magnet, except with the magnetic field set to zero so that these gels experienced no alignment.

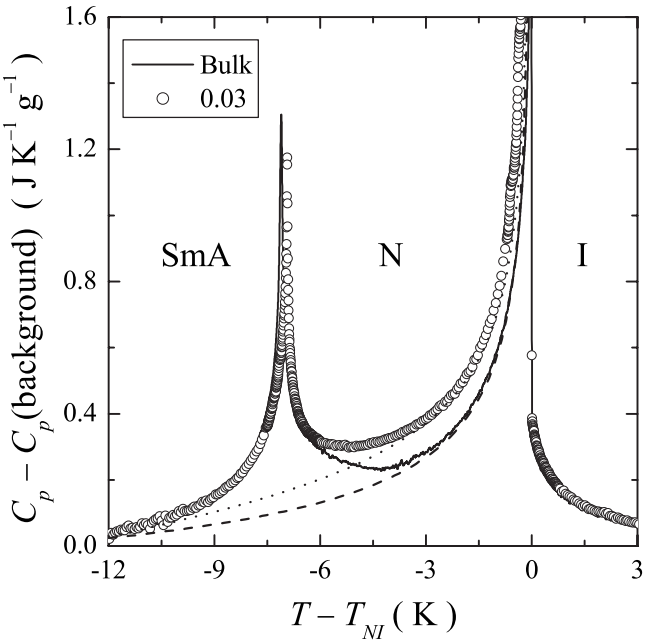

FIG. 1. Comparison of the specific heat for pure 8CB (taken from Ref. [12]) with that for 8CB confined in an aligned gel with an aerosil density ρ_S of 0.03. See text for a discussion of C_p(background). The dashed lines represent the C_p(baseline) variation expected for the *N-I* peak in the absence of a *N*-Sm*A* transition. The transition temperature T_{NI} is taken to be the high-temperature limit of *N-I* two-phase coexistence.

III. RESULTS AND ANALYSIS

A. Calorimetric results

The heat capacity of a liquid crystal consists of two distinct contributions—a large and weakly temperature-dependent background heat capacity C_p(background) that represents the result expected for a nonmesogenic organic liquid of comparable molar mass and a phase transition contribution, due in the case of 8CB to the *N-I* and *N*-Sm*A* phase transitions. Figure 1 shows this phase transition part C_p-C_p(background) for pure 8CB [12] and for 8CB confined in an aligned gel with ρ_S=0.03. The value of C_p(background), in J K^{-1} g^{-1}, for pure 8CB is well represented over the 290–320 K range by $0.6011+(4.17\times10^{-3})T$, and very similar linear backgrounds are obtained for all the 8CB+sil samples.

The smooth dashed curve underlying the *N*-Sm*A* heat capacity peak represents C_p(baseline)-C_p(background), where C_p(baseline) is the C_p variation expected for the *N-I* peak in the absence of an *N*-Sm*A* transition. The excess heat capacity associated with the *N*-Sm*A* transition is given by

$$\Delta C_p(NA) = C_p - C_p(\text{baseline}). \tag{3}$$

It is obvious from a series of plots like that shown in Fig. 1 that the nematic wing of the *N-I* heat capacity peak varies with the sil density ρ_S whereas the isotropic wing above T_{NI} shows an excellent overlay of C_p(pure) and C_p(sil). This behavior differs from that observed for random 8CB+sil gels [12] where the *N-I* wings coincide for pure 8CB and the 8CB+sils on both sides of T_{NI}. See Ref. [27] for further details of the C_p behavior in the *N-I* region for 8CB in aligned gels. The C_p(baseline) curves for aligned 8CB+sils and pure 8CB differ by a quantity linear in $\Delta T=T-T^*_{NA}$, where T^*_{NA} is the effective *N*-Sm*A* critical temperature: $C_p(\text{baseline,sil})=C_p\,(\text{baseline,pure})+B_1+B_2T$. Values of B_1, B_2, and T^*_{NA} are given in Table I for all the investigated 8CB+sil samples together with the mean void size l_0 for each gel.

Figure 2 shows $\Delta C_p(NA)$ over a 3-K wide region about T^*_{NA} for pure 8CB and all six aligned 8CB+sil gels. The $\Delta C_p(NA)$ data for the two random gel samples are not shown, but they agree very well with the corresponding $\Delta C_p(NA)$ data given in Ref. [12]. It is clear from Fig. 2 that the $\Delta C_p(NA)$ peaks for the aligned gel samples are truncated at a finite maximum value h_M and have an integrated enthalpy $\delta H_{NA}=\int\Delta C_p(NA)dT$ that varies with ρ_S. Values of h_M and δH_{NA} are given in Table I and these quantities will be compared to those for random 8CB+sil gels in Sec. III D.

TABLE I. Summary of several features of the calorimetric results for the nematic to smectic-*A* phase transition for 8CB in six aligned and two random (unaligned) gels formed in 8CB+aerosil systems. The units are grams of silica per cm^3 8CB for the aerosil density ρ_S, nm for the void size l_0, K for the effective critical temperature T^*_{NA}, J K^{-1} g^{-1} and J K^{-2} g^{-1}, respectively for the baseline parameters B_1 and B_2 (see text), J g^{-1} for the integrated enthalpy δH_{NA}, and J K^{-1} g^{-1} for the maximum heat capacity h_M. In all cases, g represents the grams of 8CB liquid crystal.

Sample	ρ_S	l_0	T^*_{NA}	B_1	B_2	δH_{NA}	h_M
Pure 8CB	0	∞	306.890	0	0	0.80	
Aligned	0.030	222	306.295	0.059	0.0116	0.69	1.04
	0.050	133	305.929	0.057	0.0108	0.62	0.84
	0.070	95	305.858	0.046	0.0091	0.59	0.77
	0.100	67	306.143	0.051	0.0089	0.58	0.51
	0.130	51	306.160	0.041	0.0066	0.52	0.40
	0.150	44	306.100	0.033	0.0039	0.51	0.39
Unaligned	0.050	133	306.101	0	0	0.60	0.88
	0.130	51	306.294	0	0	0.44	0.29

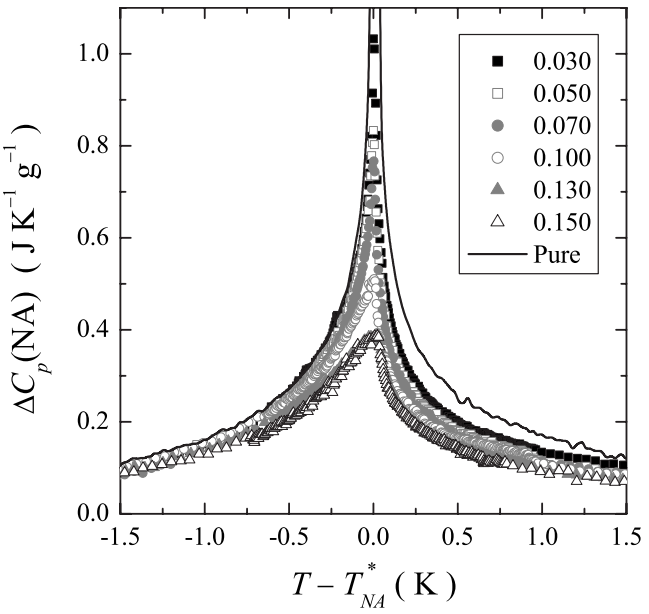

FIG. 2. Overlay of the specific heat associated with the *N*-Sm*A* transition for pure 8CB and six aligned 8CB+aerosil gel samples. The inset indicates the aerosil densities ρ_S for these gels, and the effective critical temperatures T^*_{NA} are given in Table I.

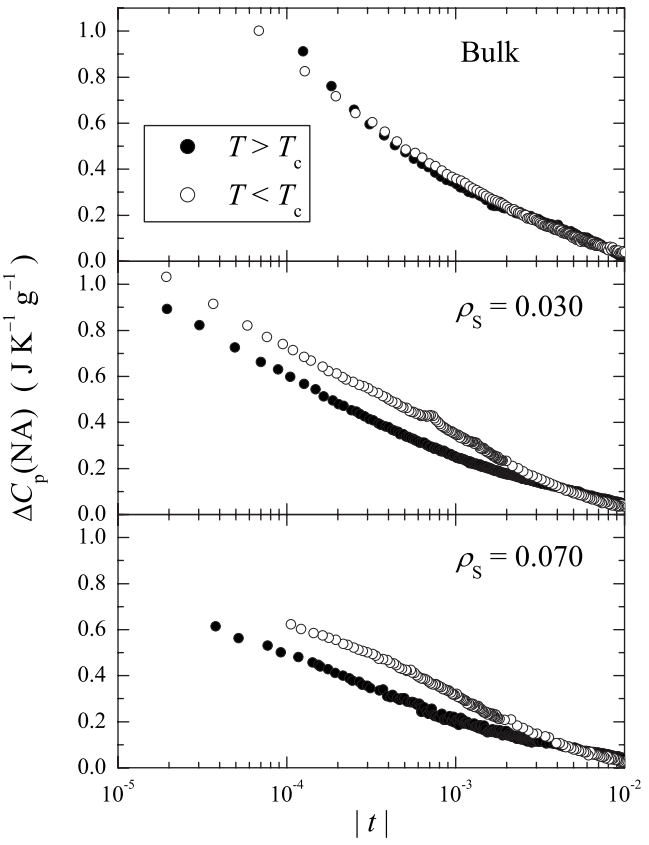

FIG. 3. Semilog plots of the excess specific heat associated with the *N*-Sm*A* transition as a function of reduced temperature t for pure 8CB and two aligned gels with aerosil densities ρ_S of 0.030 and 0.070. Power-law fits to the aligned gel data were carried out for $|t| < |t|_{\max} = 0.005$.

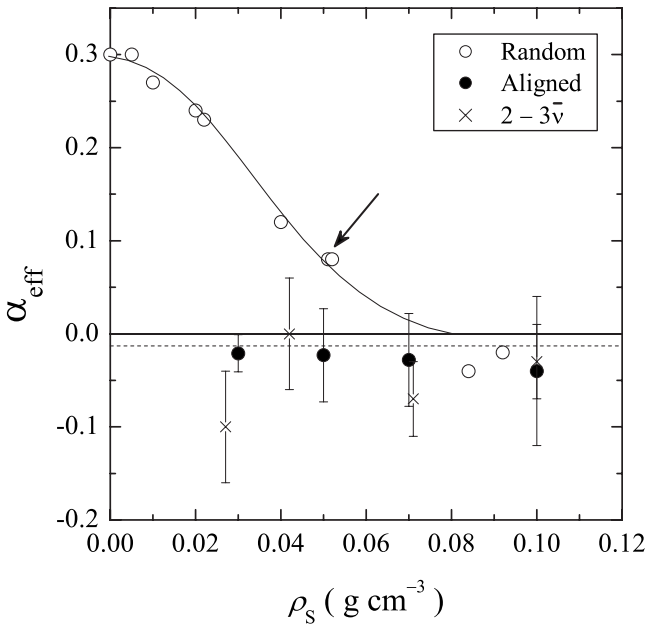

FIG. 4. The aerosil density dependence of the critical heat capacity exponent α for the *N*-Sm*A* transition in 8CB+sil aligned gels (solid circles) and 8CB+sil random gels (open circles, from Refs. [12,16] plus one marked by an arrow from the present study). The $\times$ symbols are α predicted by hyperscaling applied to the correlation volume exponent $3\bar{\nu}$ obtained from data in Ref. [19]. The dashed line indicates the value of $\alpha_{XY} = -0.013$.

B. Critical analysis

The principal objective of the present study is to characterize the critical fluctuation behavior of $\Delta C_p(NA)$ for aligned gel samples. A critical exponent analysis has been carried out using the usual power law form with corrections-to-scaling terms [10,12],

$$\Delta C_p(\mathrm{NA}) = A^{\pm}|t|^{-\alpha}(1 + D^{\pm}|t|^{0.5}) + B_C, \tag{4}$$

where $t = (T - T^*_{NA})/T^*_{NA}$ is the reduced temperature and B_C is a temperature-independent term arising from the singular free energy.

Figure 3 provides a qualitative demonstration that the dependence of $\Delta C_p(NA)$ on $|t|$ for 8CB in aligned gels differs greatly from that of $\Delta C_p(NA)$ for pure 8CB. This figure also shows that the critical exponent α for aligned 8CB+sils must be close to zero (since $\ln|t|$ corresponds to the $\alpha \to 0$ limit). The least-squares fits with Eq. (4) were carried out only for sils in the so-called soft gel regime [12,17,21] where $\rho_S \leqslant 0.1$. This corresponds to the range of sil densities studied with x-ray scattering [19]; and in practical terms fitting the samples with $\rho_S = 0.13$ and 0.15 would be difficult in any case due to the extent of truncation and rounding near T^*_{NA} for those samples. The fits were of good quality and residual plots, not shown, do not reveal any significant structure. The parameter values obtained from fitting $\Delta C_p(NA)$ with Eq. (4) are given in Table II.

As shown in Fig. 4, the behavior of the critical exponent α as a function of ρ_S is dramatically different for aligned gels and random gels. In the case of random gels, α varies gradu-

TABLE II. Least-squares parameter values for a fit with Eq. (4) to the specific heat peak $\Delta C_p(NA)$ associated with the N-SmA phase transition in aligned 8CB+aerosil samples. The fit parameters B_C and $A^{\pm}$ are given in J K^{-1} g^{-1} units, and the parameters $D^{\pm}$ are dimensionless. The range of reduced temperatures used for these fits is from $|t|_{\max}=0.005$ to $\pm t_{\min}$.

ρ_S	T^*_{NA} (K)	α	B_C	A^+	A^-/A^+	D^+	D^-	$10^5 t_{\min}$	χ^2_ν
0.030	306.295	-0.021 ± 0.02	8.892	−10.121	0.978	−0.488	−0.079	+3.72/−8.83	1.257
0.050	305.929	-0.025 ± 0.05	6.879	−8.019	0.972	−0.547	−0.094	+4.48/−13.3	1.239
0.070	305.858	-0.028 ± 0.05	5.702	−6.781	0.965	−0.630	−0.022	+7.12/−16.1	1.313
0.100	306.143	-0.040 ± 0.08	2.834	−3.268	1.081	0.530	−0.572	+22.6/−32.7	1.868

ally with ρ_S, changing smoothly from the pure 8CB value to approximately the 3D-XY value, $\alpha_{XY}=-0.013$ [28], when ρ_S is ~0.1. For the aligned gels, the α values are independent of ρ_S and agree within their error limits with α_{XY}. Another indication of XY-like critical behavior for $\Delta C_p(NA)$ of aligned gels is the amplitude ratio A^-/A^+. The theoretical value of this ratio for the 3D-XY model is 0.971 [29], and the A^-/A^+ values in Table II agree very well with this except for the sample with $\rho_S=0.100$. The correction-to-scaling coefficients $D^{\pm}$ are less well behaved. However, these correction terms only play a role in the fit for $|t|$ values near $|t|_{\max}=0.005$ and do not influence the asymptotic α value.

C. Comparison with x-ray scattering results: Hyperscaling and two-scale-factor universality

The critical behavior of $\Delta C_p(NA)$ for 8CB in aligned gels is completely consistent with that of the correlation lengths obtained in a recent x-ray study [19]. The x-ray scattering profile is characterized by two correlation lengths $\xi_\parallel=\xi_{\parallel 0}t^{-\nu_\parallel}$ and $\xi_\perp=\xi_{\perp 0}t^{-\nu_\perp}$, one parallel and one perpendicular to the nematic director (i.e., normal to the smectic layers and in the layers, respectively). Values reported for the critical exponents $\nu_\parallel$ and $\nu_\perp$ are given in Table III. It is clear that these values are essentially independent of the aerosil density ρ_S and distinct from the values for pure 8CB, which is the same pattern of critical behavior observed for the exponent α.

As discussed below, there is a close connection between the leading singularity in $\Delta C_p(NA)$ and the correlation volume given by

$$\xi_\parallel\xi_\perp^2=(\xi_{\parallel 0}\xi_{\perp 0}^2)t^{-\nu_\parallel-2\nu_\perp}=(\xi_{\parallel 0}\xi_{\perp 0}^2)t^{-3\bar{\nu}}. \tag{5}$$

Shown in Fig. 5 is a log-log plot of $\xi_\parallel\xi_\perp^2$ versus the reduced temperature t for the four x-ray samples of aligned 8CB+aerosils. Several features should be noted. Fits with Eq. (5) yield correlation volume exponents $3\bar{\nu}$ that are all close to the 3D-XY value 2.013 [28], as shown in Table III. These $3\bar{\nu}$ values are also in excellent agreement with the $\nu_\parallel+2\nu_\perp$ values obtained from Ref. [19], as they must be. Furthermore, the magnitude of $\xi_\parallel\xi_\perp^2$ is almost the same for all ρ_S values, while the mean void volume, l_0^3, rapidly decreases from 1.5×10^{10} to 3.0×10^8 Å^3 as ρ_S increases from 0.027 to 0.100. Finally, the correlation volume for 8CB in aligned gels is larger at small reduced temperatures than that for pure 8CB. The latter behavior is mostly due to the behavior of $\xi_\perp$. At $t=10^{-2}$, both $\xi_\parallel$ and $\xi_\perp$ values for sil samples are almost the same as the pure 8CB values. But at $t=10^{-4}$, $\xi_\parallel$(sil) $\approx1.25\xi_\parallel$(pure LC), and $\xi_\perp$(sil) $\approx2.0\xi_\perp$(pure LC).

The connection between the critical behavior of $\Delta C_p(NA)$ and $\xi_\parallel\xi_\perp^2$ involves two theoretical relationships: (a) hyperscaling [31]

$$2-\alpha=3\bar{\nu} \quad \text{or } 2-\alpha-3\bar{\nu}=0, \tag{6}$$

(b) two-scale-factor universality [32]

$$(R_\xi^+)^3=\alpha(\rho_{\mathrm{LC}}A^+/k_B)(\xi_\parallel\xi_\perp^2)t^{2-\alpha} \tag{7a}$$

$$=\alpha(\rho_{\mathrm{LC}}A^+/k_B)(\xi_{\parallel 0}\xi_{\perp 0}^2)t^{2-\alpha-3\bar{\nu}} \tag{7b}$$

$$=\alpha(\rho_{\mathrm{LC}}A^+/k_B)(\xi_{\parallel 0}\xi_{\perp 0}^2), \tag{7c}$$

where the two-scale-factor quantity R_ξ^+ has a common constant value for all members of a given universality class. Hyperscaling has been shown to hold for pure LCs even when the exponents do not correspond to those from any known universality class [10], and Table III shows that hyperscaling is obeyed within the error bounds for aligned

TABLE III. Critical correlation length parameters for 8CB in aligned gels [19] compared with the fit parameters for $\Delta C_p(NA)$ from calorimetry. The x-ray data are characterized by $\xi_\parallel=\xi_{\parallel 0}t^{-\nu_\parallel}$ and $\xi_\perp=\xi_{\perp 0}t^{-\nu_\perp}$ leading to a correlation volume $\xi_\parallel\xi_\perp^2=\xi_{\parallel 0}\xi_{\perp 0}^2t^{-3\bar{\nu}}$. In three cases, the aerosil densities ρ_S for C_p data ($\rho_S=0.030, 0.070, 0.100$) are very close to the x-ray values. For the case of $\rho_S=0.042$, the α and A^+ values given here were interpolated between the values for $\rho_S=0.030$ and 0.050 in Table II. The typical uncertainties are ±0.02 for the $\nu_\parallel$ and $\nu_\perp$ values [19] and ±0.04 for $3\bar{\nu}$ obtained from a power-law fit to the correlation volume. The exponents for pure 8CB ($\rho_S=0$) come from Refs. [12,30]. R_ξ^+ is the two-scale-factor universal quantity defined in Eq. (7a).

ρ_S	$-\alpha$	$-A^+$	$\nu_\parallel$	$\nu_\perp$	$\nu_\parallel+2\nu_\perp$	$3\bar{\nu}$	$2-\alpha-3\bar{\nu}$	R_ξ^+
0	−0.30	−0.076	0.67	0.51	1.69	1.69	0.01	0.308
0.027	0.021	10.121	0.73	0.70	2.13	2.10	−0.079	0.389
0.042	0.023	8.98	0.74	0.65	2.04	2.00	0.023	0.378
0.071	0.028	6.781	0.75	0.66	2.07	2.07	−0.042	0.433
0.10	0.040	3.268	0.73	0.65	2.03	2.02	0.020	0.344

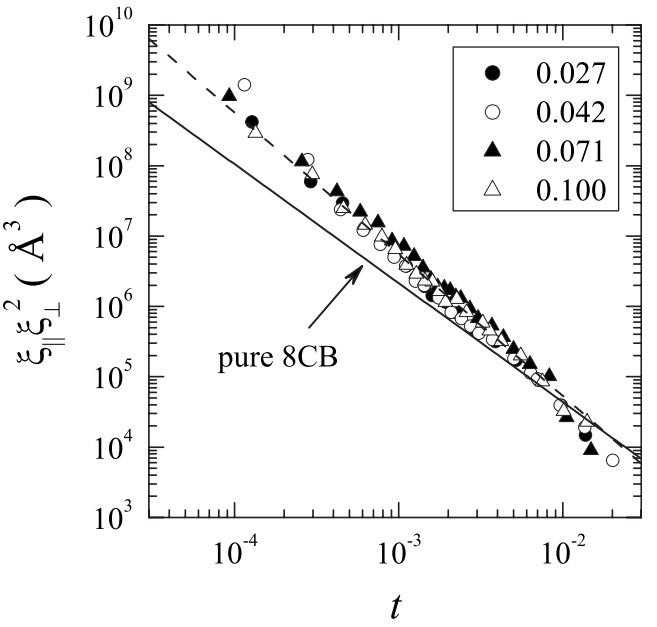

FIG. 5. Critical behavior of the correlation volume $\xi_{\parallel}\xi_{\perp}^2$ for aligned 8CB+aerosil samples [19]. Solid line represents the behavior of $\xi_{\parallel}\xi_{\perp}^2$ for pure 8CB [30], and the dashed line shows the 3D-*XY* slope $3\nu_{XY}=2.013$.

8CB+aerosils, where the exponents α and $3\bar{\nu}$ are close to 3D-*XY* values. Clearly, the concept of two-scale universality depends on hyperscaling being valid so that $t^{2-\alpha-3\bar{\nu}}=1$ for all t. In order to take into account a very weak temperature dependence in R_{ξ}^{+} for these sils due to the fact that the least squares $3\bar{\nu}$ is not exactly equal to $2-\alpha$, the R_{ξ}^{+} values given in Table III were obtained by averaging values given by Eq. (7a) over the reduced temperature range $5\times10^{-4}<t<5\times10^{-3}$. All the individual values for a given sil density lie within ±0.02 of the average value. The listed values of R_{ξ}^{+} for aligned 8CB+aerosils are fairly close to the *XY* value of 0.3606 [32].

D. *N*-Sm*A* transition characteristics

In addition to the behavior of the critical exponent α described above, there are several other features of the $\Delta C_p(NA)$ peaks that deserve mention. The dependencies of the effective critical temperature T_{NA}^{*}, the maximum peak value h_M, and the integrated enthalpy δH_{NA} on the aerosil density ρ_S of aligned gels are described here and compared to those for random gels.

The sil density dependence of T_{NA}^{*} is shown in Fig. 6 for aligned and random gels. In both cases, there is a distinctive nonmonotropic variation $T_{NA}^{*}(\rho_S)$ in the soft gel regime (ρ_S less than ~0.1). A very similar variation has been observed for $T_{NI}(\rho_S)$ [12,27], and the dip in both T_{NA}^{*} and T_{NI} is more pronounced for aligned gels than for random gels. The complex character of the shifts in transition temperatures has been discussed qualitatively for random gels in terms of a crossover from random-dilution behavior at low ρ_S to elastic-strain behavior at large ρ_S [12,33], and this interpretation presumably applies to the aligned gels as well.

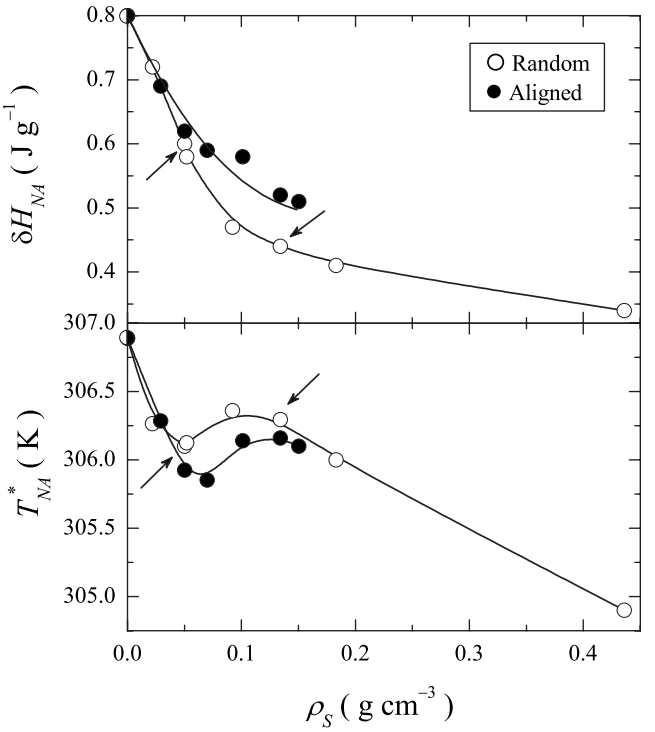

FIG. 6. The aerosil density dependence of the effective *N*-Sm*A* critical temperature T_{NA}^{*} and the integrated enthalpy for the *N*-Sm*A* transition of 8CB in aligned gels (solid circles) and unaligned random gels (open circles, from Ref. [12] plus two points marked by arrows from the present study).

The truncation of the $\Delta C_p(NA)$ peaks for aligned gels, given by the maximum peak values h_M in Table I, is quantitatively very similar to that reported for random gels [12]. This agreement is reasonable since the truncation is well described as a finite-size-scaling effect where the cutoff length scale is the mean void size l_0 [17,21], and small-angle scattering studies indicate that the alignment process does not appreciably restructure the gel on the length scale of l_0 [18]. The variation with ρ_S of the integrated *N*-Sm*A* enthalpy δH_{NA} of aligned gels is qualitatively similar to that for random gels but differs somewhat in magnitude, as shown in Fig. 6. An attempt to describe $\delta H_{NA}(\rho_S)$ for random gels in terms of finite-size scaling was not very successful [17,21] and such a description has not been attempted for aligned gels.

IV. DISCUSSION AND CONCLUSIONS

As described above, the effects of the aligned aerosil gel on the *N*-Sm*A* critical behavior are twofold. First, the thermodynamically sharp transition behavior is destroyed, leading to a truncation of the *N*-Sm*A* heat capacity peak that can be understood as a finite-size effect with a cutoff length scale l_0. Second, the pseudocritical fluctuations are altered in a way that cannot be interpreted in terms of finite-size effects. Power-law analysis of the data for aligned samples successfully describes C_p on both sides of the transition over a broad range of reduced temperatures, revealing critical exponents

and amplitude ratios markedly different from those of either random samples or bulk 8CB. Similarly, the x-ray scattering results display altered critical exponents that are fully consistent with the C_p findings.

To understand how the N-SmA transition for 8CB in aligned gels can be affected throughout the transition region, even at reduced temperatures where the smectic correlations are small compared with l_0, requires a brief review of the character of the N-SmA transition in pure LCs [34]. The SmA order parameter is $|\psi|\exp(ikz+\phi)$, which is like the superconductor order parameter Ψ for an XY normal-superconductor transition. However, for LCs there is significant coupling between the smectic positional and the nematic orientational order that complicates the N-SmA critical behavior. The nematic order is described by a tensor Q_{ij} that can be characterized by the scalar magnitude S on short length scales and a nematic director ("headless" vector) $\hat{n}$ on long length scales. There are two types of nematic-smectic coupling. The first of these is S-$|\psi|$ coupling arising from a term $C|\psi|^2\delta S$ in the free energy, where δS is the change in the nematic order induced by the formation of smectic layers; and the perturbing effect of this coupling depends on the magnitude of $C^2\chi_N$, where χ_N is the nematic susceptibility [34]. The second type of coupling involves the coupling of fluctuations $\delta\hat{n}$ in the nematic director $\hat{n}$ with the phase ϕ of the smectic order parameter.

The effect of S-$|\psi|$ coupling is well understood, and it causes a crossover from second order to tricritical behavior that is clearly established for pure LCs [10]. When the nematic range T_{NI}-T_{NA} is large, χ_N is small at T_{NA} (since S is almost saturated) and the N-SmA transition is second order with $\alpha=\alpha_{XY}$. As the nematic range shrinks, S-$|\psi|$ coupling grows and the transition crosses over to first order via a tricritical point with $\alpha=0.5$. Unfortunately, the detailed effects of $\delta\hat{n}$-ϕ coupling on the character of a N-SmA transition are still not well established theoretically [35], but this coupling is the cause of the critical anisotropy $\nu_\parallel > \nu_\perp$ observed in the behavior of the correlation lengths [34,35]. For pure 8CB, the nematic range is fairly small (7.0 K [12]) and both S-$|\psi|$ and $\delta\hat{n}$-ϕ coupling effects are strong, as shown by the exponent values given in Table III. For pure LCs with very wide nematic ranges (45–190 K), S-$|\psi|$ coupling is absent and the critical behavior of $\Delta C_p(NA)$, the correlation volume $\xi_\parallel\xi_\perp^2$, and the smectic susceptibility σ is XY-like although there is still a small residual anisotropy $\Delta\nu \equiv \nu_\parallel - \nu_\perp > 0$ [36].

The influence of aerosil gels on the N-SmA critical behavior of 8CB is substantial. As shown by the $\alpha(\rho_S)$ variation in Fig. 4, the S-$|\psi|$ coupling effect is "turned off" by the aerosil but in different ways for random and aligned gels. For 8CB+sil random gels and other LC+sil random gels [14,15], the variation of α with ρ_S is quite gradual and α varies smoothly from α_{pure} to α_{XY} as ρ_S varies from 0 to ~0.1. In contrast to this, samples of 8CB in aligned gels exhibit $\alpha \approx \alpha_{XY}$ for all ρ_S values investigated. This ρ_S independence of the critical behavior in aligned gels is also true for the x-ray correlation length exponents $\nu_\parallel$ and $\nu_\perp$ [19]. In the context of contributions to the free energy, this suppression of S-$|\psi|$ coupling implies a reduction in $C^2\chi_N$. As mentioned earlier, theory indicates that the gel introduces both random fields that couple to the smectic order and orientational fields conjugate to the nematic order. These orientational fields are clearly different in aligned and random gels. However, we hypothesize that in both cases they act to reduce the nematic susceptibility, leading to the approach to XY critical behavior. For a given gel density, aligned gels are clearly more effective than random gels in promoting this reduction. Furthermore, since the correlation length anisotropy is markedly reduced—$\Delta\nu$ is 0.16 for pure 8CB but only 0.085 ± 0.04 for 8CB+sil aligned gels—the $\delta\hat{n}$-ϕ coupling is also presumably greatly reduced for 8CB in aligned gels compared to that in pure 8CB.

In spite of the very small critical anisotropy $\Delta\nu$ and the XY-like behavior of both the critical heat capacity $\Delta C_p(NA)$ and the correlation volume $\xi_\parallel\xi_\perp^2$, there is one transition feature that is distinctly non-XY. The smectic susceptibility exponent γ has a density independent value for the four x-ray samples of 8CB in aligned gels, ranging from 1.53 to 1.56 with an average value of 1.545 ± 0.05 [19], and this differs greatly from the 3D-XY value of 1.317 [28]. This large γ value for 8CB in aligned gels resembles those observed in pure LCs with intermediate nematic ranges [10] rather than pure 8CB ($\gamma=1.26\pm0.06$ [30]) or pure LCs with very wide nematic ranges ($\gamma=\gamma_{XY}$ [36]), but the reason for such a γ value is unclear.

There are several unresolved issues that deserve attention. Experimentally, it would be of considerable interest to explore the crossover behavior for the critical exponents of 8CB in aligned gels with densities between $\rho_S=0$ (pure 8CB) and the lowest aerosil density investigated here or with x-rays ($\rho_S\approx0.03$). The percolation threshold for gelation is $\rho_S^0\sim0.01$ [12,16]. For $0<\rho_S<\rho_S^0$, there is no network gel structure and small clusters of aerosil particles are dispersed as solutes in a LC solvent phase. In this non-gel regime, the critical exponents are very similar to those in pure 8CB [16]. The interesting region for study would be 8CB in aligned gels with densities $\rho_S^0<\rho_S<0.03$, assuming that robust alignment can be achieved for such low density samples. Theoretically, there are two questions of interest. How does an aligned gel act to completely turn off the S-$|\psi|$ coupling effect and greatly reduce the $\delta\hat{n}$-ϕ coupling? Why is an aligned gel much more effective than a random gel in changing the critical N-SmA behavior? Presumably, aligned and random gels affect long wavelength nematic fluctuations, and hence χ_N, differently; however, it should be noted that neither have any substantial effect on the width of the nematic range.

ACKNOWLEDGMENTS

This work was supported at WPI by the NSF under Grant No. DMR-0092786 and at Johns Hopkins by the NSF under Grant No. DMR-0134377.

[1] R. J. Birgeneau, H. Yoshizawa, R. A. Cowley, G. Shirane, and H. Ikeda, Phys. Rev. B **28**, 1438 (1983).
[2] M. H. W. Chan, K. I. Blum, S. Q. Murphy, G. K. S. Wong, and J. D. Reppy, Phys. Rev. Lett. **61**, 1950 (1988).
[3] X.-l. Wu, W. I. Goldburg, M. X. Liu, and J. Z. Xue, Phys. Rev. Lett. **69**, 470 (1992); T. Bellini, N. A. Clark, C. D. Muzny, L. Wu, C. W. Garland, D. W. Schaefer, and B. J. Oliver, *ibid.* **69**, 788 (1992); T. Bellini, L. Radzihovsky, J. Toner, and N. A. Clark, Science **294**, 1074 (2001).
[4] R. Eidenshink and W. H. de Jeu, Electron. Lett. **27**, 1195 (1991).
[5] M. Kreuzer, T. Tschudi, W. H. de Jeu, and R. Eidenshink, Appl. Phys. Lett. **62**, 1712 (1993).
[6] Y. W. Zhou, M. Jaroniec, and R. K. Gilpin, J. Colloid Interface Sci. **185**, 39 (1997).
[7] G. Puchkovskaya, Yu. Reznikov, A. Yakubov, O. Yaroshchuk, and A. Glushchenko, J. Mol. Struct. **404**, 121 (1997).
[8] B. Zhou, G. S. Iannacchione, C. W. Garland, and T. Bellini, Phys. Rev. E **55**, 2962 (1997); H. Haga and C. W. Garland, *ibid.* **56**, 3044 (1997).
[9] T. Bellini, N. A. Clark, V. Degiorgio, F. Mantegazza, and G. Natale, Phys. Rev. E **57**, 2996 (1998).
[10] C. W. Garland and G. Nounesis, Phys. Rev. E **49**, 2964 (1994).
[11] L. Radzihovsky and J. Toner, Phys. Rev. B **60**, 206 (1999).
[12] G. S. Iannacchione, C. W. Garland, J. T. Mang, and T. P. Rieker, Phys. Rev. E **58**, 5966 (1998).
[13] R. L. Leheny, S. Park, R. J. Birgeneau, J. L. Gallani, C. W. Garland, and G. S. Iannacchione, Phys. Rev. E **67**, 011708 (2003).
[14] P. S. Clegg, C. Stock, R. J. Birgeneau, C. W. Garland, A. Roshi, and G. S. Iannacchione, Phys. Rev. E **67**, 021703 (2003).
[15] M. Ramazanoglu, S. Larochelle, C. W. Garland, and R. J. Birgeneau, Phys. Rev. E **75**, 061705 (2007); H. Haga and C. W. Garland, *ibid.* **56**, 3044 (1997).
[16] M. Marinelli, A. K. Ghosh, and F. Mercuri, Phys. Rev. E **63**, 061713 (2001).
[17] G. S. Iannacchione, S. Park, C. W. Garland, R. J. Birgeneau, and R. L. Leheny, Phys. Rev. E **67**, 011709 (2003).
[18] D. Liang, M. A. Brothwick, and R. L. Leheny, J. Phys.: Condens. Matter **16**, S1989 (2004).
[19] D. Liang and R. L. Leheny, Phys. Rev. E **75**, 031705 (2007).
[20] B. Jacobsen, K. Saunders, L. Radzihovsky, and J. Toner, Phys. Rev. Lett. **83**, 1363 (1999); K. Saunders, B. Jacobsen, L. Radzihovsky, and J. Toner, J. Phys.: Condens. Matter **12**, A215 (2000).
[21] G. S. Iannacchione, Fluid Phase Equilib. **222**, 177 (2004).
[22] A. Roshi, S. Barjami, G. S. Iannacchione, D. Paterson, and I. McNulty, Phys. Rev. E **74**, 031404 (2006).
[23] H. Yao and C. W. Garland, Rev. Sci. Instrum. **69**, 172 (1998).
[24] D. Sharma and G. S. Iannacchione, J. Chem. Phys. **126**, 094503 (2007).
[25] C. C. Retsch, I. McNulty, and G. S. Iannacchione, Phys. Rev. E **65**, 032701 (2002).
[26] R. Bandyopadhyay, D. Liang, R. H. Colby, J. L. Harden, and R. L. Leheny, Phys. Rev. Lett. **94**, 107801 (2005).
[27] F. Cruceau, D. Liang, R. L. Leheny, and G. S. Iannacchione, Liq. Cryst. **35**, 1061 (2008).
[28] J. Zinn-Justin, Phys. Rep. **344**, 159 (2001).
[29] C. Bervillier, Phys. Rev. B **34**, 8141 (1986).
[30] D. Davidov, C. R. Safinya, M. Kaplan, S. S. Dana, R. Schaetzing, R. J. Birgeneau, and J. D. Litster, Phys. Rev. B **19**, 1657 (1979).
[31] P. M. Chaikin and T. C. Lubensky, *Principles of Condensed Matter Physics* (Cambridge University Press, Cambridge, 1995).
[32] D. Stauffer, M. Ferer, and M. Wortis, Phys. Rev. Lett. **29**, 345 (1972); C. Bagnuls and C. Bervillier, Phys. Rev. B **32**, 7209 (1985).
[33] M. Caggioni, A. Roshi, S. Barjami, F. Mantegazza, G. S. Iannacchione, and T. Bellini, Phys. Rev. Lett. **93**, 127801 (2004).
[34] P. G. de Gennes and J. Prost, *The Physics of Liquid Crystals*, 2nd ed. (Oxford University Press, Oxford, 1993), Sec. 10.1.
[35] B. S. Andereck, Int. J. Mod. Phys. B **9**, 2139 (1995).
[36] C. W. Garland, G. Nounesis, M. J. Young, and R. J. Birgeneau, Phys. Rev. E **47**, 1918 (1993).